Dynamical traffic light strategy in the Biham-Middleton-Levine model

Jia-Rong Xie,[1] Rui Jiang,[2,*] Zhong-Jun Ding,[3] Qi-Lang Li,[4] and Bing-Hong Wang[1,5,†]

[1]*Department of Modern Physics, University of Science and Technology of China, Hefei, 230026, PRC*

[2]*School of Engineering Science, University of Science and Technology of China, Hefei, 230026, PRC*

[3]*School of Transportation Engineering, Hefei University of Technology, Hefei, 230009, PRC*

[4]*Department of Mathematics and Physics, Anhui University of Architecture, Hefei, 230601, PRC*

[5]*Complex System Research Center, University of Shanghai for Science and Technology and Shanghai Academy of System Science, Shanghai, 200093, PRC*

(Received 19 November 2012; revised manuscript received 31 January 2013; published 20 February 2013)

In this paper, we study dynamical traffic light strategies in the Biham-Middleton-Levine traffic flow model. The strategies use local vehicular information to control urban traffic, which take into account the interaction of vehicles traveling in different directions via considering their dynamical spatial configuration. Simulations find out two strategies, in which local information at nearby sites is used. The two strategies perform much better than the alternating strategy. Under these two strategies, vehicles can self-organize into a new intermediate state with band structure. The analytical solutions of velocity of this state have been presented, which are in good agreement with simulations.

DOI: 10.1103/PhysRevE.87.022812 PACS number(s): 89.40.−a, 05.50.+q, 64.60.Cn, 05.70.Ln

I. INTRODUCTION

Traffic flow in urban network is complex and contains rich information, which might be utilized to enhance network performance. Simple discrete cellular automate (CA) approach has been used to model network traffic [1–5]. The Biham-Middleton-Levine (BML) model is the first CA model to simulate urban traffic [6], which has attracted much attention from physicists and has been studied widely [7–14].

In the BML model, each site can be seen as a traffic crossing, controlled by a traffic light. In the seminal work of BML [6], two traffic light strategies have been studied: an alternating one and a random one. In the alternating strategy, on odd (even) steps, every traffic light switches simultaneously into green for northbound (eastbound) vehicles. This strategy has a period of two time steps, and the maximum velocity of a vehicle is $1/2$.[1] In the random strategy, all vehicles attempt to move one lattice site forward at all time steps. A vehicle moves forward if its front site is empty and no other vehicle competes for the site [see Fig. 1(a)]. If two vehicles from different directions compete for the same empty site, the traffic light will randomly select one vehicle to move.

Brockfeld *et al.* have studied the impact of global traffic light control strategies in city networks [15]. They found that the capacity of the network strongly depends on the period of the traffic light. Effect of traffic light periods in the BML model has also been studied, and a phase separation phenomenon has been found [16,17]. These traffic light strategies are static and independent of current status of nearby sites. Gershenson has studied several traffic light strategies in city networks [18]. They found that using simple rules, traffic lights are able to self-organize and adapt to changing traffic conditions.

The spatial correlation of urban traffic is strong. Vehicles will interact with each other directly or indirectly. This paper studies dynamical traffic light strategies in the BML model. The strategies use local vehicular information to control urban traffic, which take into account the interaction of vehicles traveling in different directions via considering their dynamical spatial configuration.

This paper is organized as follows. In Sec. II, the model is presented, and the dynamical strategies have been studied. It is shown that when local information at nearby sites is considered, the dynamical strategies will perform much better than the alternating strategy. Section III shows a new intermediate state in the model. We have investigated average velocity in the state analytically, which is in good agreement with simulations. Section IV studies effect of turning vehicles in the model. The conclusions are given in Sec. V.

II. MODEL AND STRATEGIES

The initial distribution of vehicles in the model is the same as in the original BML model: There are two species of vehicles, eastbound and northbound ones, distributed on a two-dimensional periodic square lattice with size $L \times L$. For each site, the probabilities that it is occupied by an eastbound vehicle, a northbound vehicle, or is empty, are equal to $\rho/2$, $\rho/2$, and $1-\rho$, respectively.

The dynamical strategy is as follows. Similar to the random strategy, all vehicles attempt to move one lattice site forward at all time steps. A vehicle moves if its front site is empty and no other vehicle competes for the site. If two vehicles from different directions compete for the same empty site, the traffic light in the empty site will select one vehicle according to the condition of nearby sites [see Fig. 1(b)].

The traffic light decides which vehicle to move depending on the direction and relative positions of nearby vehicles. For example, if there is an eastbound vehicle on the southwest site of the competed site, the traffic light in the competed site

*rjiang@ustc.edu.cn

†bhwang@ustc.edu.cn

[1]Note that in most literature, the unit of velocity is site per period when this strategy is adopted. Therefore, the maximum velocity is 1.

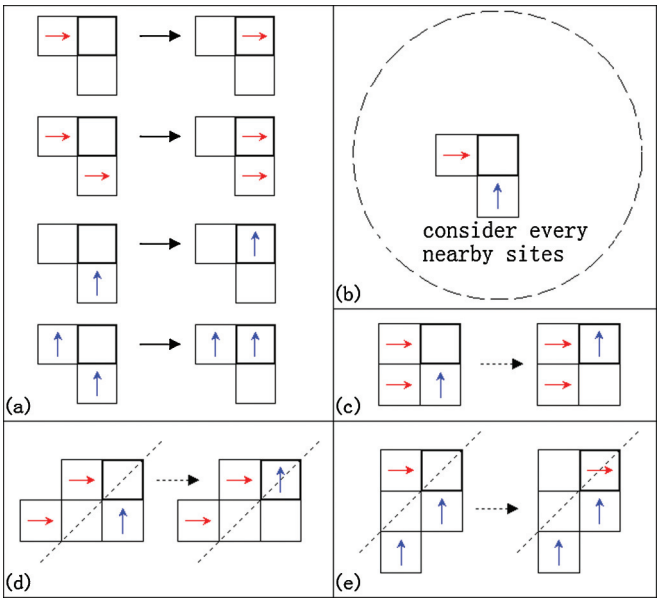

FIG. 1. (Color online) Sketch of our model. We focus on the overstriking site. (a) If there is no vehicle competing for its front empty site, a vehicle moves. (b) If two vehicles compete for an empty site, traffic light in the competed site will select one of them depending on condition of nearby sites. (c) Example of the interaction. (d) and (e) Parameters $s_{i,j}$ should be symmetrical in properties.

should tend to let the northbound vehicle move, because if the northbound vehicle moves, the front site of the eastbound vehicle at southwest site will be empty. Thus, this eastbound vehicle could move at the next step [see Fig. 1(c)]. If the vehicle on the southwest site of the competed site is northbound, the traffic light at the competed site should tend to have an opposite decision.

For simplicity, this paper combines the impact of each site linearly, as follows, for the competed site (x,y):

$$f_{x,y} = \sum_{i,j} s_{i,j} V_{x+i,y+j}, \tag{1}$$

where $s_{i,j}$ are a series of parameters, and $V_{x+i,y+j}$ denotes the state of site $(x+i,y+j)$. If it is occupied by an eastbound (northbound) vehicle, $V_{x+i,y+j} = 1(-1)$; $V_{x+i,y+j} = 0$ if it is empty. The traffic light decides according to the sign of $f_{x,y}$. If $f_{x,y} > 0\,(<0)$, the eastbound (northbound) vehicle moves to the competed site; if $f_{x,y} = 0$, one of them is chosen randomly with equal probability.

The two directions should be symmetrical in properties. For instance, in a situation that the traffic light at (x,y) lets the northbound vehicle go when there is an eastbound vehicle at position $(x-2,y-1)$ [Fig. 1(d)], it should let the eastbound vehicle go when there is a northbound vehicle at position $(x-1,y-2)$ [Fig. 1(e)]. Therefore, parameters $s_{i,j}$ should be symmetrical in properties, $s_{i,j} = s_{j,i}$. Thus, Eq. (1) could be written as

$$f_{x,y} = \sum_{i} s_{i,i} V_{x+i,y+i} + \sum_{i<j} s_{i,j} (V_{x+i,y+j} + V_{x+j,y+i}). \tag{2}$$

In the special case that $s_{i,j} = 0, \forall i,j$, the dynamical strategy reduces to the random strategy. As shown in Fig. 2, the random

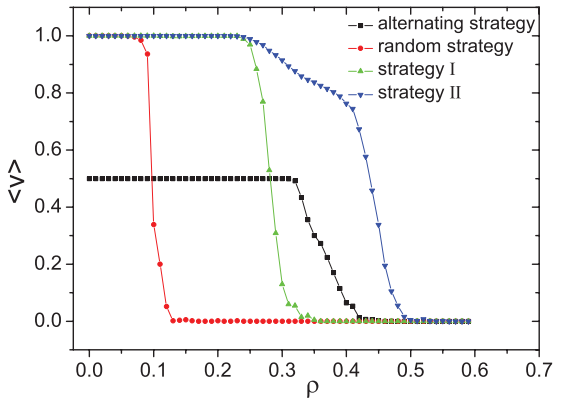

FIG. 2. (Color online) Average velocity against density under some traffic light strategies. System size $L = 128$.

strategy performs better than the alternating strategy only in the very low-density range. The density threshold of the transition from free flow state into jam is much smaller than that in the alternating strategy.

Now we try to find the site that affects the traffic flow most significantly. To this end, we study one-parameter strategies in which only one parameter is nonzero. Note that since the decision of traffic light depends only on the sign of f, the absolute value of the parameter does not matter. For example, if other parameters are all set to 0, $s_{-1,-1} = 1$ and $s_{-1,-1} = 2$ are the same strategy, but $s_{-1,-1} = 1$ and $s_{-1,-1} = -1$ are different strategies.

In the simulations, the average velocity is obtained by averaging over 400 independent initial realizations. As shown in Fig. 3(a), the strategy in which

$$s_{-1,-1} = -1 \tag{3}$$

is the best, and it is named as strategy I. However, as can be seen in Fig. 2, although strategy I performs much better than the random strategy, the density threshold is still remarkably smaller than that of alternating strategy.

Next we study two-parameter strategies, in which there is another nonzero parameter apart from $s_{-1,-1} = -1$. As mentioned above, since the decision of traffic light depends only on the sign of f, sometimes the absolute value of the other nonzero parameter does not matter when it is in a certain range. For example, if the other nonzero parameter is $s_{-2,-1}$, and it is in the range $-0.5 < s_{-2,-1} < 0$, then its absolute value does not matter.

As shown in Fig. 3(b), in the two-parameter strategy family, the strategies in which

$$s_{-1,-1} = -1 \quad s_{-2,-1} = -0.1 \tag{4}$$

and

$$s_{-1,-1} = -1 \quad s_{-3,-2} = -0.1 \tag{5}$$

perform better than others in terms of density threshold.[2] Since the two strategies perform almost the same, we only need to show one of them. Here, we choose strategy $s_{-1,-1} =$

[2]Note that the average velocity of strategy $s_{-1,-1} = -1, s_{-2,-2} = -0.1$ is slightly larger in the density range $0.25 < \rho < 0.375$.

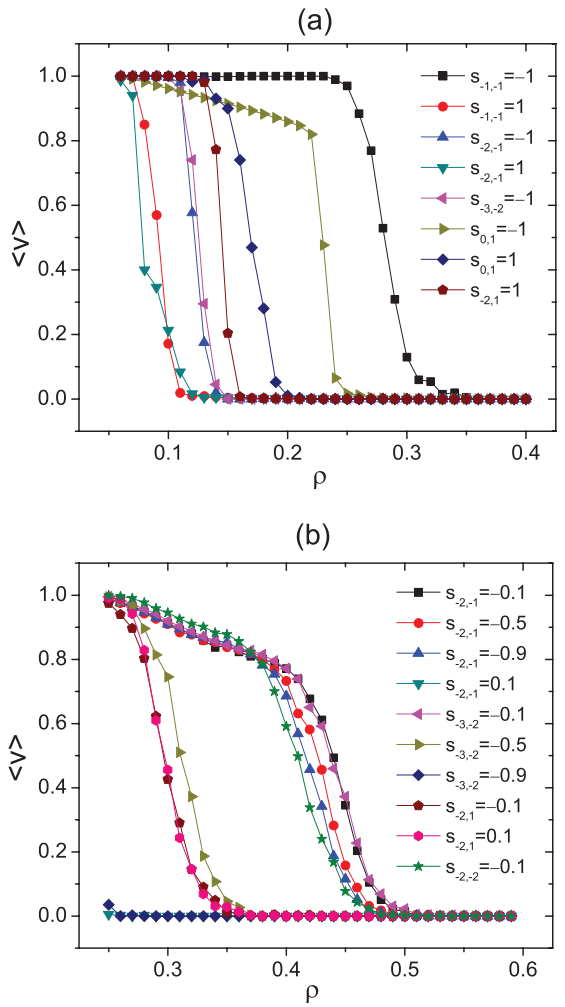

FIG. 3. (Color online) Some typical results of average velocity against density under different (a) one parameter, (b) two parameter traffic light strategies. System size $L = 128$. We have simulated with many other parameters of $s_{i,j}$ (not shown), and none of them performs better than the best strategies shown here.

-1, $s_{-2,-1} = -0.1$ and name it as strategy II.[3] As can be seen in Fig. 2, strategy II performs much better than the alternating strategy; the density threshold becomes remarkably larger than that of alternating strategy.[4]

III. INTERMEDIATE STATE

As can be seen from Fig. 2, under strategy II the average velocity gradually decreases when the density exceeds $\rho \approx 0.25$ before the system transits into jam at $\rho \approx 0.45$. In this density range, an intermediate state could be observed

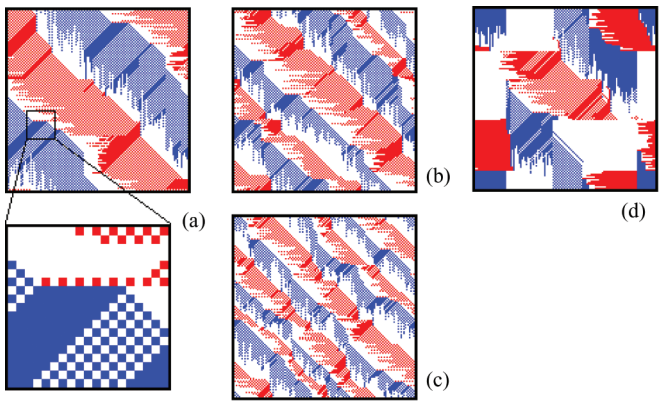

FIG. 4. (Color online) Typical configurations of intermediate state. (a), (b), and (c) show typical configurations of two-band, four-band, and six-band states, respectively. System size $L = 128$. The density (a) $\rho = 0.45$, (b) $\rho = 0.4$, and (c) $\rho = 0.35$. (d) Typical configuration of the intermediate state shown by the arrow described in the legend of Fig. 7. System size $L = 128$, the density $\rho = 0.48$.

as shown in Figs. 4(a)–4(c), 5, and 6. The system could evolve into band structure [19], in which some rows (columns) have more vehicles than others, and these vehicles block vehicles of the other direction.[5] The band number depends on system density, system size, and initial configuration. When the system density is low, the band number could be large, as shown in Fig. 5. With the increase of density, the band number tends to decrease, and two-band, four-band, and six-band patterns could be observed in a wide range of system density [Figs. 4(a)–4(c)]. However, we have not observed states with more bands in the large density range for system size $L = 128$ and 256 in the 100 realizations in the simulations (i.e., the appearance probability of patterns with more bands is smaller than $1/100$). When we carried out simulations with larger system size $L = 512$, we have occasionally observed an eight-band pattern in the large density range, as shown in Fig. 6. However, the appearance probability of an eight-band pattern is small (it appears 1 time in 100 realizations at density $\rho = 0.35$).

To study the average velocity $\bar{v}$ of intermediate state, we consider one site (x, y). Since the appearance probability of eight or more bands is very small at a large density range (in particular when system size is not very large), we present results of two-band, four-band, and six-band states, and states with more bands could be analyzed similarly. First, we study the two-band state. We denote the number of northbound (eastbound) vehicles on column x (row y) as $N_{\uparrow,x}$ ($N_{\rightarrow,y}$). If we only consider column x and row y, the situation changes into the model similar to that studied in Ref. [20]. Each vehicle needs two time steps to go across the crossing site (x, y). It takes $2(N_{\uparrow,x} + N_{\rightarrow,y})$ time steps for all these vehicles to go across this crossing site. Therefore,

$$\tau = \max[2(N_{\uparrow,x} + N_{\rightarrow,y}), L]. \quad (6)$$

[3] As mentioned before, here $s_{-2,-1} = -0.1$ (or $s_{-3,-2} = -0.1$) does not matter provided $-0.5 < s_{-2,-1} < 0$ ($-0.5 < s_{-3,-2} < 0$).

[4] We have tested many other two-parameter strategies not including $s_{-1,-1} = -1$, and none of them performs better than strategy II. However, unfortunately, presently we could not prove that the best strategy including $s_{-1,-1} = -1$ performs better than any other two-parameter strategy not including $s_{-1,-1} = -1$, which is a challenge topic in the future work.

[5] Similar intermediate state could be observed under strategy $s_{-1,-1} = -1$, $s_{-3,-2} = -0.1$.

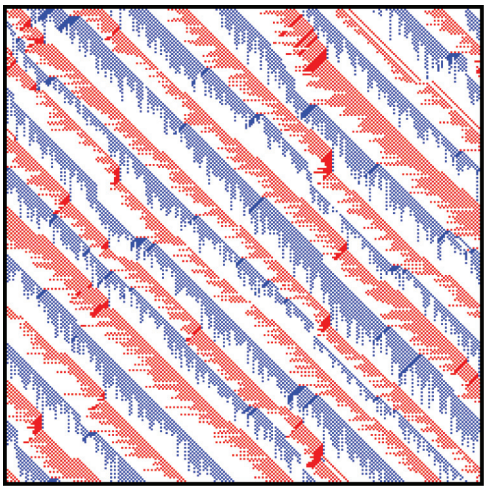

FIG. 5. (Color online) Typical configurations of intermediate state with 12 bands. System size $L = 256$, the density $\rho = 0.27$.

Here, τ is the average time needed for one vehicle to move L sites. Therefore, the average velocity $\bar{v}'$ is

$$\bar{v}' = \frac{L}{\tau} = \frac{L}{\max[2(N_{\uparrow,x} + N_{\rightarrow,y}), L]} = \min\left[\frac{L}{2(N_{\uparrow,x} + N_{\rightarrow,y})}, 1\right]. \quad (7)$$

For the whole system, the average velocity $\bar{v}_2$ is determined by the smallest $\bar{v}'$ and it could be approximated by

$$\bar{v}_2 = \min\left[\frac{L}{2(N_{\max,\uparrow} + N_{\max,\rightarrow})}, 1\right], \quad (8)$$

in which $N_{\max,\uparrow} = \max_{x=1}^{L}\{N_{\uparrow,x}\}$, $N_{\max,\rightarrow} = \max_{y=1}^{L}\{N_{\rightarrow,y}\}$.

For each site of column x, the probability that it is occupied by a northbound vehicle is $\rho/2$. The distribution of $N_{\uparrow,x}$ is

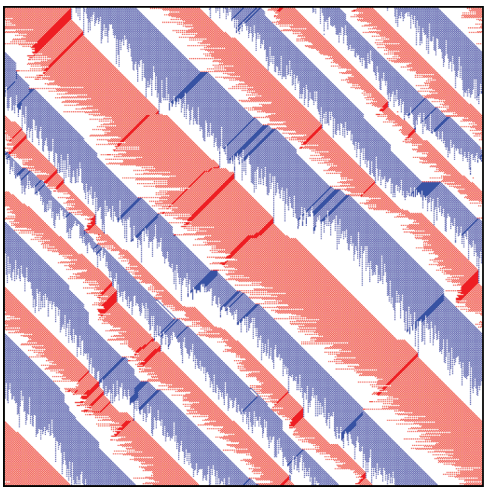

FIG. 6. (Color online) Typical configurations of intermediate state with eight bands. System size $L = 512$; the density $\rho = 0.35$.

thus a binomial one,

$$P_{L,2}(N_{\uparrow,x} = i) = C_L^i\left(\frac{\rho}{2}\right)^i\left(1 - \frac{\rho}{2}\right)^{L-i}, \quad (9)$$

$$P_{L,2}(N_{\uparrow,x} \leqslant n) = \sum_{i=0}^{n} P_{L,2}(N_{\uparrow,x} = i). \quad (10)$$

We assume that the number of northbound vehicles of each column are independent, thus

$$P_{L,2}(N_{\max,\uparrow} \leqslant n) = \prod_{x=1}^{L} P_{L,2}(N_{\uparrow,x} \leqslant n) = (P_{L,2}(N_{\uparrow,x} \leqslant n))^L, \quad (11)$$

$$P_{L,2}(N_{\max,\uparrow} = n) = P_{L,2}(N_{\max,\uparrow} \leqslant n) - P_{L,2}(N_{\max,\uparrow} \leqslant n-1). \quad (12)$$

Similarly, distribution of $N_{\max,\rightarrow}$ could be obtained. If we ignore the correlation of numbers of vehicles of each row and column, the distribution of $N_{\max,\rightarrow} + N_{\max,\rightarrow}$ could be calculated by

$$P_{L,2}(N_{\max,\uparrow} + N_{\max,\rightarrow} = N) = \sum_{n=0}^{N} P_{L,2}(N_{\max,\uparrow} = n)P_{L,2}(N_{\max,\rightarrow} = N - n). \quad (13)$$

From Eqs. (8)∼(13), we can obtain

$$\bar{v}_2 = \sum_{N=0}^{[L/2]}\sum_{n=0}^{N} X_2(n, N-n) + \sum_{N=[L/2]+1}^{2L}\frac{L}{2N}\sum_{n=0}^{N} X_2(n, N-n), \quad (14)$$

with

$$X_2(n, N-n) = [P_{L,2}(n) - P_{L,2}(n-1)] \times [P_{L,2}(N-n) - P_{L,2}(N-n-1)],$$

and $P_{L,2}(x) = [\sum_{i=0}^{x} C_L^i(\rho/2)^i(1-\rho/2)^{L-i}]^L$.

Similarly, for a four-band state, the average velocity

$$\bar{v}_4 = \min \times \left\{\frac{L}{2(N_{\max,\uparrow,1} + N_{\max,\uparrow,2} + N_{\max,\rightarrow,1} + N_{\max,\rightarrow,2})}, 1\right\}, \quad (15)$$

in which, $N_{\max,\uparrow,1}$ is the maximum number of northbound vehicles of each column in northbound band 1, and $N_{\max,\uparrow,2}$, $N_{\max,\rightarrow,1}$, $N_{\max,\rightarrow,2}$ have similar meaning. For each site of column x, the probability that it is occupied by a northbound vehicle in band 1 is approximated by $\rho/4$, one has

$$P_{L,4}(N_{\uparrow,x,1} = i) = C_L^i\left(\frac{\rho}{4}\right)^i\left(1 - \frac{\rho}{4}\right)^{L-i}. \quad (16)$$

Similar to Eqs. (10)∼(12), we have $P_{L,4}(N_{\uparrow,x,1} \leqslant n)$, $P_{L,4}(N_{\max,\uparrow,1} \leqslant n)$, $P_{L,4}(N_{\max,\uparrow,1} = n)$. $N_{\max,\uparrow,2}$, $N_{\max,\rightarrow,1}$, $N_{\max,\rightarrow,2}$ could be calculated similarly. We ignore the correlation of numbers of vehicles of the four

bands

$$P_{L,4}(N_{\max,\uparrow,1}+N_{\max,\uparrow,2}+N_{\max,\rightarrow,1}+N_{\max,\rightarrow,2}=N)$$
$$=\sum_{n_1=0}^{N}\sum_{n_2=0}^{N-n_1}\sum_{n_3=0}^{N-n_1-n_2}P_{L,4}(N_{\max,\uparrow,1}=n_1)$$
$$\times P_{L,4}(N_{\max,\uparrow,2}=n_2)P_{L,4}(N_{\max,\rightarrow,1}=n_3)$$
$$\times P_{L,4}(N_{\max,\rightarrow,2}=N-n_1-n_2-n_3). \quad (17)$$

Consequently, $\bar{v}_4$ could be obtained

$$\bar{v}_4=\sum_{N=0}^{[L/2]}\sum_{n_1=0}^{N}\sum_{n_2=0}^{N-n_1}\sum_{n_3=0}^{N-n_1-n_2}X_4$$
$$+\sum_{N=[L/2]+1}^{4L}\frac{L}{2N}\sum_{n_1=0}^{N}\sum_{n_2=0}^{N-n_1}\sum_{n_3=0}^{N-n_1-n_2}X_4, \quad (18)$$

with

$$X_4=X_4(n_1,n_2,n_3,n_4=N-n_1-n_2-n_3)$$
$$=\prod_{i=1}^{4}[P_{L,4}(n_i)-P_{L,4}(n_i-1)],$$

and $P_{L,4}(x)=[\sum_{i=0}^{x}C_L^i(\rho/4)^i(1-\rho/4)^{L-i}]^L$.

Similarly, the average velocity in a six-band state is

$$\bar{v}_6=\sum_{N=0}^{[L/2]}\sum_{n_1=0}^{N}\sum_{n_2=0}^{N-n_1}\sum_{n_3=0}^{N-n_1-n_2}\sum_{n_4=0}^{N-n_1-n_2-n_3}\sum_{n_5=0}^{N-n_1-n_2-n_3-n_4}X_6$$
$$+\sum_{N=[L/2]+1}^{6L}\frac{L}{2N}\sum_{n_1=0}^{N}\sum_{n_2=0}^{N-n_1}\sum_{n_3=0}^{N-n_1-n_2}$$
$$\times\sum_{n_4=0}^{N-n_1-n_2-n_3}\sum_{n_5=0}^{N-n_1-n_2-n_3-n_4}X_6, \quad (19)$$

with

$$X_6=X_6(n_1,n_2,n_3,n_4,n_5,n_6=N-n_1-n_2-n_3-n_4-n_5)$$
$$=\prod_{i=1}^{6}[P_{L,6}(n_i)-P_{L,6}(n_i-1)],$$

and $P_{L,6}(x)=[\sum_{i=0}^{x}C_L^i(\rho/6)^i(1-\rho/6)^{L-i}]^L$.

Figure 7 compares the analytical results with the simulation ones in system with sizes $L=128$ and $L=256$. Here, simulation results of each realization have been shown. One can see that the analytical solutions are in good agreement with simulation results.

Finally, as shown by the arrow in Fig. 7, there exists another intermediate state under strategy II. A typical configuration of this state is shown in Fig. 4(d) [19]. The evolution of this state is quite complex and analytical investigation of its average velocity needs to be carried out in future work, which might be a challenge.

IV. EFFECT OF TURNING VEHICLES

This section studies the effect of turning vehicles in the model. In real urban traffic patterns, the changing of the motion directions via the turnings at crossroads can be essential because it leads to spatial correlations between the vehicle flow along the different directions.

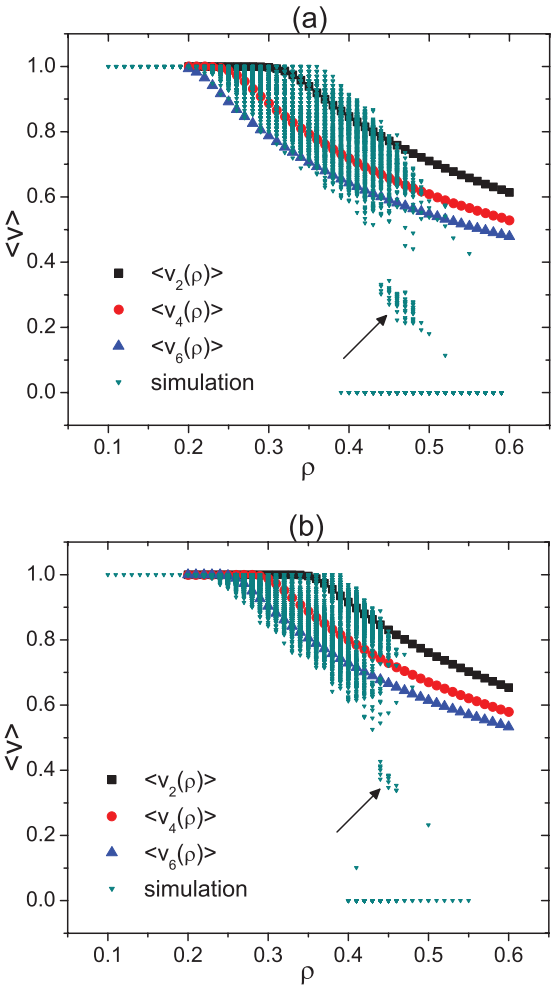

FIG. 7. (Color online) Simulation results and analytical solutions under strategy II. For each density we simulate 400 independent realizations. System sizes: (a) $L=128$; (b) $L=256$.

We introduce turning vehicles as in model A in Ref. [21], in which a vehicle moving preferentially toward east (north) moves toward east (north) with probability $1-\gamma$ and toward

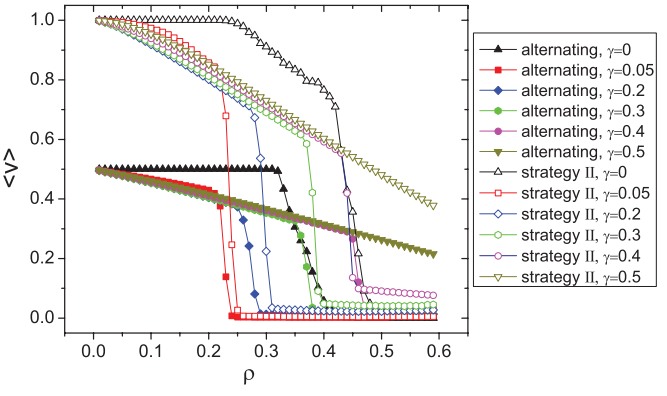

FIG. 8. (Color online) Effect of turning vehicles on the average velocity under strategy II and alternating strategy. System size, $L=128$.

north (east) with probability γ. Due to symmetry, it is enough to study the range $0 \leqslant \gamma \leqslant 1/2$. Figure 8 shows the average velocity versus system density under different values of γ. It can be seen that with the introduction of turning, the intermediate state disappears. The jamming phase also disappears because the average velocity in the phase becomes larger than zero and it increases with the increase of γ. The density threshold first decreases and then increases with the increase of γ. When γ reaches 0.5, the phase transition disappears. Strategy II still performs better than the alternating strategy (in terms of density threshold), provided γ is not very close to 0.5. When γ reaches 0.4, the density thresholds of the two strategies become almost identical.

V. CONCLUSION

To summarize, this paper has studied dynamical traffic light strategies in the Biham-Middleton-Levine traffic flow model, in which traffic light determines which vehicle to move when two vehicles compete for an empty site, based on dynamical spatial configuration of vehicles nearby the site.

We have studied one-parameter and two-parameter strategies. It is found that in the one-parameter strategy family, the density threshold of the best strategy is still remarkably smaller than that of the alternating strategy. In the two-parameter strategy family, we find two strategies. They perform almost the same and better than others in terms of density threshold, which becomes remarkably larger than that of alternating strategy. Under the two two-parameter strategies, vehicles can self-organize into two new kinds of intermediate states. In one of the states, the system exhibits band structure. The analytical solutions of velocity of this state have been presented, which are in good agreement with simulations. In our future work, to find whether the density threshold could be further increased, strategies involving more parameters will be studied.

Although the BML model is a simplified urban traffic model, our result is expected to shed some light on real-world control strategies for traffic lights. Specifically, if traffic flow situations in nearby road sections were taken into account in traffic light control strategy, the system performance might be enhanced. Further investigations are needed in the future work.

Finally, we would like to mention that, recently, game theory has been introduced into traffic flow studies to solve conflicts when two or more vehicles or pedestrians compete for an empty space. For instance, Perc has introduced the evolutionary game between neighboring agents in the Biham-Middleton-Levine model and he found that a traffic flow seizure is induced [22]. The evolutionary game has also been introduced into random walk to study immigration behaviors [23] and into unidirectional pedestrian flow to study its phase transition behaviors [24]. Ji *et al*. have studied conflict between pedestrians and vehicles in a signalized intersection [25] as well as conflict in pedestrian flow [26] by using a majority-based game. Tanimoto *et al*. [27] and Zheng and Cheng [28] have introduced game theory to study the evacuation process.

Since real urban traffic networks are composed of both signalized intersections and unsignalized ones, we will study the coupled effect of traffic light strategies and evolutionary game (which deals with conflict at unsignalized intersections) on traffic flow in our future work.

ACKNOWLEDGMENTS

We are thankful for the comments of two anonymous referees, which enabled us to find the incorrect statement in the original manuscript and to improve the paper. This work is funded by the National Nature Science Foundation of China (Grants No. 11275186, No. 91024026, and No. 11072239) and the Specialized Research Fund the Doctoral Program of Higher Education of China (Grant No. 20093402110032). R.J. acknowledges the support of Fundamental Research Funds for the Central Universities (Grant No. WK2320000014). The numerical calculations in this paper have been done on the supercomputing system in the Supercomputing Center of University of Science and Technology of China.

[1] D. Chowdhury, L. Santen, and A. Schadschneider, Phys. Rep. **329**, 199 (2000).
[2] D. Helbing, Rev. Mod. Phys. **73**, 1067 (2001).
[3] T. Nagtani, Rep. Prog. Phys. **65**, 1331 (2002).
[4] A. Schadschneider, Physica A **313**, 153 (2002).
[5] K. Nagel and M. Schreckenberg, J. Phys. I **2**, 2221 (1992).
[6] O. Biham, A. A. Middleton, and D. Levine, Phys. Rev. A **46**, R6124 (1992).
[7] T. Nagatani, Phys. Rev. E **48**, 3290 (1993).
[8] S. I. Tadaki and M. Kikuchi, Phys. Rev. E **50**, 4564 (1994).
[9] K. H. Chung, P. M. Hui, and G. Q. Gu, Phys. Rev. E **51**, 772 (1995).
[10] G. Q. Gu, K. H. Chung, and P. M. Hui, Physica A **217**, 339 (1995).
[11] R. M. D'Souza, Phys. Rev. E **71**, 066112 (2005).
[12] Z. J. Ding, R. Jiang, and B. H. Wang, Phys. Rev. E **83**, 047101 (2011).
[13] Z. J. Ding, R. Jiang, W. Huang and B. H. Wang, J. Stat. Mech. (2011) P06017 .
[14] Z. J. Ding, R. Jiang, M. Li, Q. L. Li, and B. H. Wang, Europhys. Lett. **99**, 68002 (2012).
[15] E. Brockfeld, R. Barlovic, and A. Schadschneider, Phys. Rev. E **64**, 056132 (2001).
[16] D. Sun, R. Jiang, and B. H. Wang, Comput. Phys. Commun. **181**, 301 (2010).
[17] Q. H. Sui, Z. J. Ding, R. Jiang, W. Huang, D. Sun, and B. H. Wang, Comput. Phys. Commun. **183**, 547 (2012).
[18] C. Gershenson, Complex Syst. **16**, 29 (2005).
[19] See Supplemental Material at http://link.aps.org/supplemental/10.1103/PhysRevE.87.022812 for videos showing evolution of these states.

[20] Y. Ishibashi and M. Fukui, J. Phys. Soc. Jpn. **65**, 2793 (1996).
[21] J. A. Cuesta, F. C. Martinez, J. M. Molera, and A. Sanchez, Phys. Rev. E **48**, R4175 (1993).
[22] M. Perc, New J. Phys. **9**, 3 (2007).
[23] X. Y. Sun, R. Jiang, Q. Y. Hao, and B. H. Wang, Europhys. Lett. **92**, 18003 (2010).
[24] Q. Y. Hao, R. Jiang, M. B. Hu, B. Jia, and Q. S. Wu, Phys. Rev. E **84**, 036107 (2011).
[25] Y. Ji *et al.*, 2008 IEEE Intelligent Vehicles Symposium (IEEE, Eindhoven, The Netherlands, 2008), p. 1191.
[26] Y. Ji *et al.*, Prog. Nat. Sci. **19**, 337 (2009) (in Chinese).
[27] J. Tanimoto, A. Hagishima, and Y. Tanaka, Physica A **389**, 5611 (2010).
[28] X. P. Zheng and Y. Cheng, Physica A **390**, 1042 (2011).